

DOI: <https://doi.org/10.24425/amm.2023.146207>CHAOYANG LI<sup>1</sup>, PENG TIAN<sup>2\*</sup>, ZHIPENG ZHAO<sup>2</sup>, XIAOHUI LIANG<sup>2</sup>,  
SHUHUAN WANG<sup>2\*</sup>, YONGLIN KANG<sup>2\*</sup>, XIAN LUO<sup>2</sup>

## EFFECT OF FINAL ROLLING TEMPERATURE ON MICROSTRUCTURE, PROPERTIES AND TEXTURE OF HOT ROLLED STRIP BY NEW ENDLESS ROLLED LINE

Donghua steel continuous casting-rolling (DSCCR) line is a new endless rolling line in which tunnel heating furnace is added before and after roughing mills to change the temperature field of slab and intermediate slab, but this change will affect the microstructure and properties of hot rolled plate. Therefore, the microstructure evolution, mechanical properties, texture analysis, hole expanding and earing test of 2.0 mm thick hot rolled plate produced by DSCCR line at different final rolling temperature of 860°C, 840°C and 820°C are studied. The results show that with the decrease of final rolling temperature, there is an obvious layered microstructure distribution along the thickness direction, and the surface coarse grain area gradually expands inward, at the same time the morphology of cementite also changed from large multi domain lamellar pearlite and long rod cementite to small single domain lamellar pearlite and short rod cementite. The engineering stress-strain curves have discontinuous yield with the yield elongation of 4-5% and the elongations are more than 35%. EBSD analysis shows that small angle grain boundaries and deformed grains increase significantly with the decrease of final rolling temperature, and are mainly distributed in fine grain area. Hole expanding and earing tests show that with the decrease of final rolling temperature, the earing performance decreased but the limiting hole expanding ratio is similar.

*Keywords:* final rolling temperature; microstructure; properties; texture; hot rolled plate

### 1. Introduction

At present, thin slab continuous casting and rolling technology has been widely promoted and applied, and the endless rolling production lines that have been put into operation include endless strip production (ESP) line, compact endless cast & rolling mill (CEM) line, Danieli universal endless & multi-mode continuous casting and rolling plant (Due-MCCR) line and Donghua steel continuous casting-rolling (DSCCR) line. In the ESP line [1], the liquid steel passes through the thin slab caster directly into the 3-stand roughing mill, and then heats by the induction heating equipment, rolls by the 5-stand finishing mills, control cools by the cooling line, and coils by the down coilers. The main difference between CEM line [2] and ESP line is that the CEM line adds a soaking device between thin slab caster and roughing mill to improve the temperature uniformity of continuous casting slab, and can free converse between batch and endless rolling modes. Unlike CEM, Due-MCCR line [3] integrate batch, semi-endless and endless rolling function in one production line.

DSCCR line [4] is a new endless rolled line characterized by the arrangement of tunnel furnace before and after roughing mills, the purpose of the first furnace is used for uniform the slab temperature, but for the second furnace, in addition to ensuring the finishing temperature, another purpose is used for uniform the intermediate temperature because it was thought that the non-uniformity of temperature distribution in the intermediate slab was corresponding to the non-uniformity of the microstructure along the thickness direction in the 1.5 mm low carbon strip [5]. Due to the differences in design ideas and equipment arrangement of these endless production lines, different effects on the microstructure and properties of hot rolled steel are inevitable. At present, relevant researches mainly focus on the advantages of endless production line [6-8] and its product [9-11], but lack of detailed research on comprehensive performance. Drawability and stretchability of low carbon steel sheets produced by the CEM process [12] and the ESP process [13] are investigated, and it is considered that these differences are related to the effects of manufacturing processes of different production lines on the mi-

<sup>1</sup> NORTH CHINA UNIVERSITY OF SCIENCE AND TECHNOLOGY, SCHOOL OF METALLURGY AND ENERGY, TANGSHAN, 063210, CHINA

<sup>2</sup> UNIVERSITY OF SCIENCE AND TECHNOLOGY BEIJING, SCHOOL OF MATERIALS SCIENCE AND ENGINEERING, BEIJING, 100083, CHINA

\* Corresponding authors: tpchbr@163.com, wshh88@ncst.edu.cn, kangyilin@ustb.edu.cn



microstructure, texture and earing behavior of steel plates. Compared with other production lines, the microstructure and performance of DSCCR products should be different due to its different production process, but there is a lack of research on its effect on the microstructure and performance of hot rolled plate. For example the 2.0 mm thickness hot rolled plate is produced by the ESP line, the temperature of the intermediate slab needs to be raised 200°C in about 21 s through the induction heating zone. However, when the same specification plate is produced by the DSCCR line, the temperature of the intermediate slab only needs to be raised 100°C in about 531 s through the tunnel heating furnace. Therefore, it is necessary to study the effect of DSCCR process on microstructure, properties and texture of low carbon mild steel.

In this paper, the effects of different final rolling temperature on the microstructure, properties and texture of hot rolled mild steel plates produced by DSCCR line were studied in detail. It will provide technical support for the production of thin and ultra-thin hot rolled steel plates by endless rolling line and provide guidance for the industrial application of hot rolled plates to replace cold rolled plate.

## 2. Materials and methods

### 2.1. Materials and production process

The chemical composition of hot rolled steel strips from the same heat is shown in TABLE 1. It is a hot-rolled low carbon steel strip of commercial and drawing qualities. Fig. 1 shows the layout and experimental process parameters of the DSCCR line in the full endless mode. The continuous casting thin slab with 95 mm thickness and 1250 mm width obtained at the casting speed of 5 m/min, the slabs were directly heated from 1010±10°C to 1080±5°C within 684 s in 1# tunnel heating furnace, and then rolled to 35 mm thickness by two stand roughing mills, heated

from 980±10°C to 1100±5°C within 531 s in 2# tunnel heating furnace, rolled to 2.0 mm thickness by the six stand finishing mills with the different final rolling temperature of 860°C (above recrystallization temperature), 840°C (Deformation induced ferrite transformation temperature region) and 820°C (the ferrite and austenite temperature region), front stage cooled, and finally the coiling process was conducted at 680±3°C. In order to ensure the final rolling temperature of 860°C, single tube descaling was used at the entrance of finishing rolling mills and the final entry temperature increased by about 30°C, others used double tube descaling. The steel sheet is cut into about 21.5 tons of steel coil by high-speed flying shear, if the weight of the steel coil is converted to the length of the batch slab, the length of the continuous casting slab is about 23 meters.

### 2.2. Samples preparation and testing

Specimens were cut from a quarter cross section of 2.0 mm thick hot rolled strip produced by DSCCR with the full endless mode according to the above parameters in Fig. 1. During the full endless rolling process, hot rolled plates about 650 tons (5 ladles) were produced and the experiments were carried out at different final rolling temperatures in the 3rd ladle with the modification process of descaling and passes cooling water. The speed of the intermediate slab and the final rolling is 0.226 m/s and 3.96 m/s. The tensile specimens with width of 20 mm and gauge length of 50 mm were processed by wire cutting and the mechanical properties were tested on a tensile testing machine. Metallographic samples were mounted, polished, and then etched in 4 vol.% nitric solution to observe the microstructure under the optical microscope (OM) and the scanning electron microscopy (SEM). The preparation for electron backscatter diffraction (EBSD) samples includes normal mechanical polishing and the electrolytic polishing with the solution containing 5 vol.%

Chemical composition of investigated materials (mass fraction, %)

TABLE 1

Steel	C	Si	Mn	P	S	Al	Fe
Required	0.030-0.045	≤0.03	0.08-0.12	≤0.017	≤0.005	0.03-0.06	balance
Actual	0.034	0.02	0.11	0.012	0.003	0.032	balance

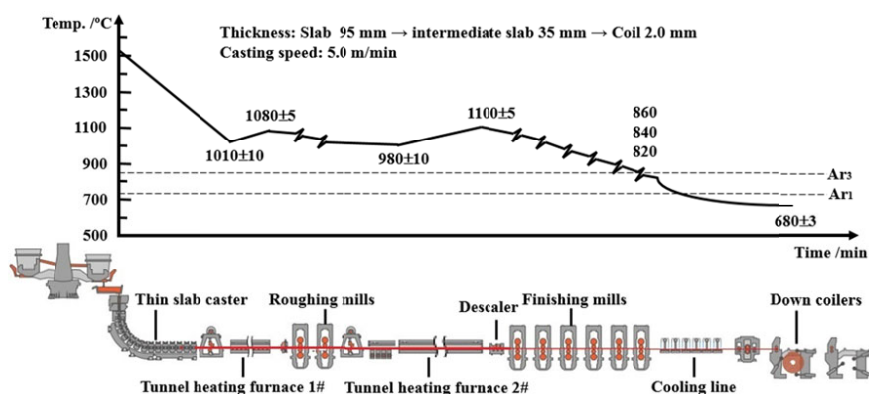


Fig. 1. Layout and experimental process diagram of the DSCCR line

perchloric acid and 95 vol.% acetic acid for 15-25 s. The earing samples are cut into discs with a diameter of 60 mm and earing tests were carried out on a universal sheet-testing machine. Hole expanding test were carried out on 120 mm × 120 mm square plate with a punching machine and a reaming testing machine. The average grain size, the thickness and the lamellar spacing of pearlite were measured by the particle size distribution calculation software of Nano Measure V 1.2 and data processing according to GB/T 6394-2017.

### 3. Results and discussions

#### 3.1. Microstructure evolution at different final rolling temperature

Fig. 2 shows the transverse microstructure along the thickness direction at different final rolling temperatures. It can be seen that there are significant differences in microstructure at different final rolling temperature because related studies show that the static transformation temperature of  $A_{r3}$  is 836°C [14] and the dynamic transformation temperature of  $A_{r3}$  is 874°C [15] when the cooling rate is 5°C/s for low carbon steel. The red rectangle corresponds to the upper surface image, and the purple rectangle corresponds to the center image. For 860°C, the average grain size of ferrite decreases gradually from 11.6  $\mu\text{m}$  on

the surface to 11  $\mu\text{m}$  at the center and without obvious interface. The grain size distribution is mainly related to the temperature gradient distribution along the thickness of intermediate slab before finishing rolled, due to the influence of heat transfer in the tunnel furnace, the temperature of the intermediate slab presents gradient distribution along the thickness direction. For 840°C, the average grain size of ferrite decreases sharply from 11.5  $\mu\text{m}$  on the surface to 7.8  $\mu\text{m}$  on the near surface, and then increases gradually to 11  $\mu\text{m}$  on the center. There is a clear interface at 85  $\mu\text{m}$  from the surface and the fine grain area is mainly related to the temperature distribution of intermediate slab. Some studies [16] suggest that deformation of ultra-fine ferrite at  $A_{e3}$  to  $T_s$  temperature is the result of deformation induced mechanism and dynamic recrystallization mechanism of ferrite. Considering that the final rolling temperature of 840°C is in the induced ferrite transformation temperature zone, it is considered that the distribution of fine grains on the near surface is related to the deformation induced ferrite transformation, and the coarse grained microstructure in the center is related to the dynamic recrystallization of austenite. For 820°C, the average grain size of ferrite decreases from 16  $\mu\text{m}$  on the surface to 9.7  $\mu\text{m}$  on the center, and there is an obvious interface at 318  $\mu\text{m}$  from the surface, mainly because the interface moves towards the center with the decrease of the final rolling temperature. At the same time, the grain size of surface ferrite is obviously larger than that at 840°C or 860°C, but the grain size of core ferrite is smaller than that at

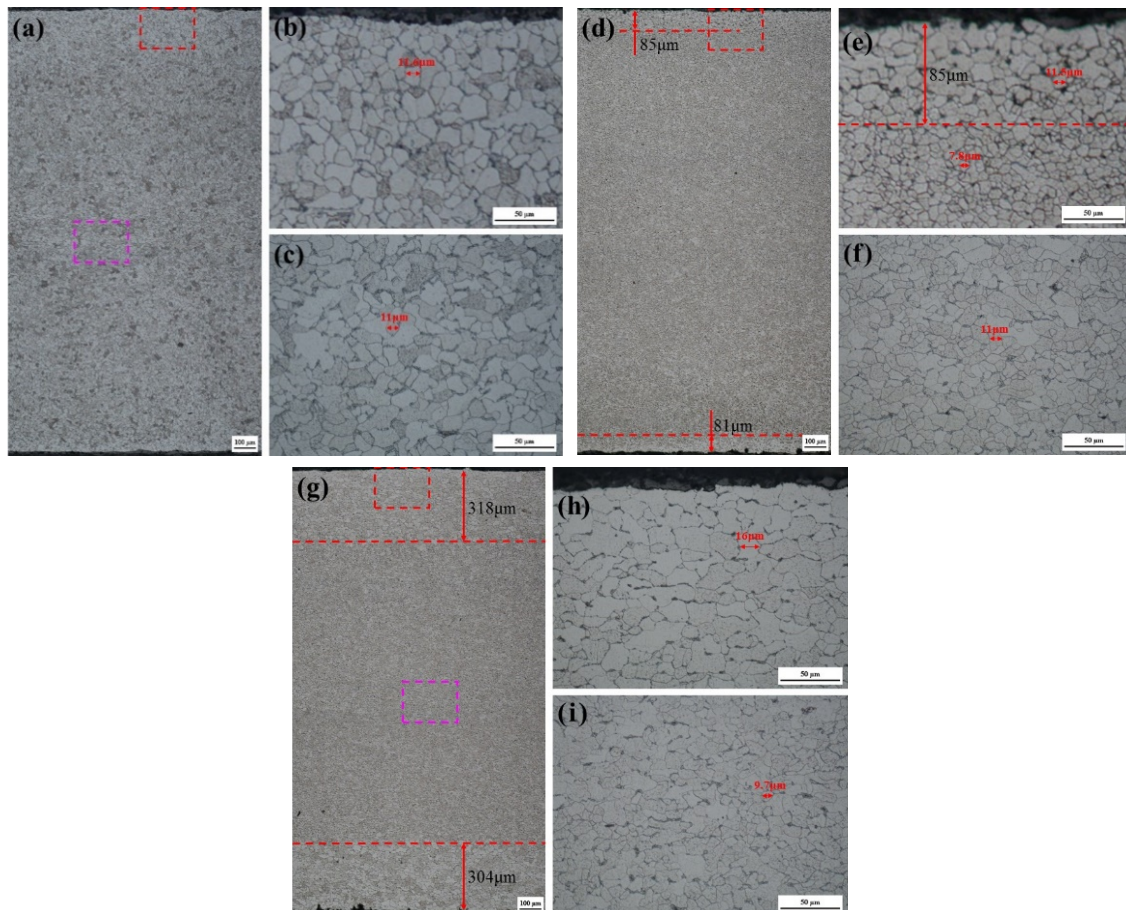


Fig. 2. Microstructure of different final rolling temperature under optical microscope: 860°C, (a), (b), (c); 840°C, (d), (e), (f); 820°C, (g), (h), (i)

840°C or 860°C. The microstructure characteristics are related to rolling in the two-phase region (ferrite and austenite) on the surface and rolling in deformation induced ferrite transformation temperature region on the inside at the final rolling pass.

In order to further analyze the microstructure evolution of cementite at different final rolling temperatures, SEM with a high resolution field emission microscope was used for in-depth and detailed observation of cementite. The cementite morphology of the thickness center is shown in Fig. 3. It can be seen that the microstructure includes ferrite, lamellar pearlite, and rod-like cementite (see the yellow arrows). For 860°C, the larger pearlite consists of several pearlite domains with different orientations, and the lamellar spacing of pearlite is about 0.15  $\mu\text{m}$  (Fig. 3a). At the same time, there are long rod-like cementite at the ferrite grain boundaries and a small amount of cementite at the ferrite corner. For 840°C, lamellar pearlite with narrow was obtained and long rod-like cementite existed at the ferritic grain boundaries (Fig. 3b). For 820°C, small lamellar pearlite with a single field is obtained, the lamellar spacing of pearlite is about 0.14  $\mu\text{m}$  (Fig. 3c), and short rod-shaped cementite exists at the ferrite grain boundaries. In addition, the outer cementite of pearlite becomes the preferred site for  $\text{Fe}_3\text{C}_{\text{III}}$ , resulting in an increase

of cementite thickness (see purple arrow in Fig. 3). The reason why the pearlite lamellar spacing is similar at different final rolling temperatures is that the pearlite transformation occurs at the laminar cooling and the cooling rate is similar. Some results [16] show that when the deformation temperature is higher than  $A_{d3}$  (Upper limit temperature of deformation-induced ferrite transformation), the austenite transforms into ferrite + lamellar pearlite, while when the deformation temperature is lower than  $A_{d3}$  but higher than  $A_{e3}$ , the nucleation rate of ferrite is greatly increased, and the austenite transforms into ferrite + lamellar pearlite + short rod cementite. Therefore, it can be inferred that the differences of microstructure and cementite morphology are closely related to the final rolling temperature.

### 3.2. Mechanical properties at different final rolling temperatures

Fig. 4 shows the engineering stress-strain curves of hot rolled plates at different final rolling temperatures. It can be seen that the engineering stress-strain curves of the hot rolled plates produced by DSCCR have discontinuous yield phenomenon, showing high upper yield strength (see the purple ellipse), stress drop and jagged yield plateau with about 4-5% yield elongation (see the red rectangle), work hardening and necking. At the same time, the stress-strain curves deviating 0°, 45° and 90° from rolling direction are different due to different mechanical values. Relevant studies [17] show that the percentage yield point extension of low carbon steel produced by CEM process is about 5%, and it needs to change the production process conditions or skin pass because the yield point phenomenon of the low carbon steel strip processed by CEM leads to stretcher strain marks, or Lüders bands, and the localized bands of plastic deformation on the surfaces [18]. However, in this experiment, no Lüders band was found on the surface of the specimen after tensile fracture, and relevant studies [15] showed that no Lüders band was found on the tensile specimen even though the yield elongation of ultra-thin hot rolled strip produced by ESP was as high as 10%.

The tensile properties of hot rolled plates at different final rolling temperatures are shown in Fig. 5. It can be seen that with

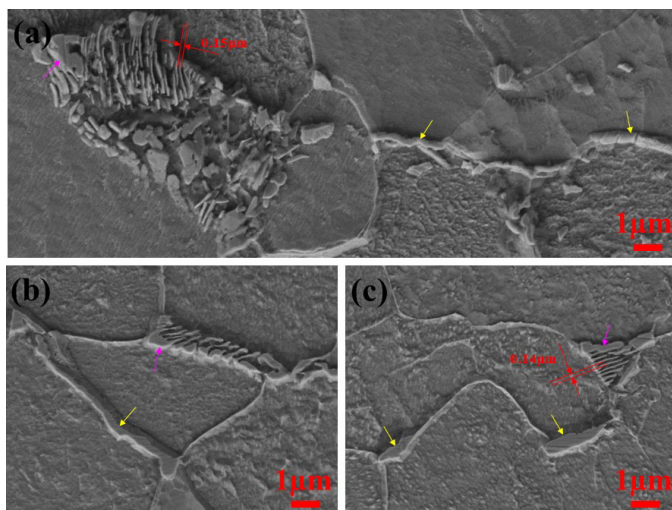


Fig. 3. Cementite morphology of the thickness center: (a) 860°C; (b) 840°C; (c) 820°C

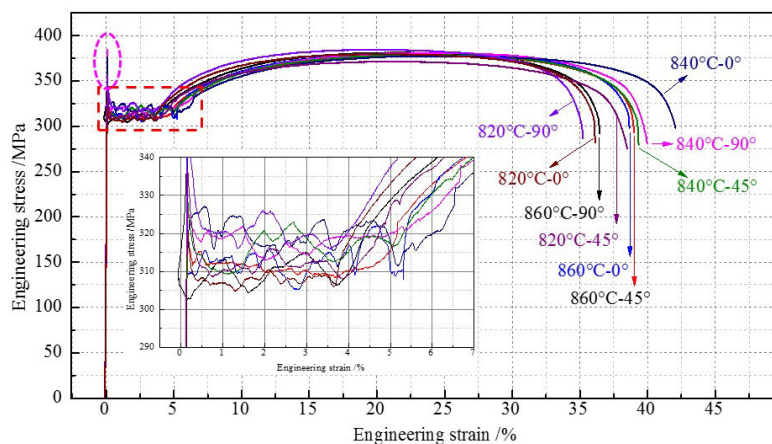


Fig. 4. Engineering stress-strain curves with different direction and final rolling temperature

the decrease of the final rolling temperature, the anisotropy of hot rolled plate is obvious, the tensile strength of longitudinal and transverse is relatively stable at 380 MPa, the yield strength of longitudinal and 45° is relatively stable at 310 MPa, and the flexural ratio is relatively stable and its elongation is the highest when the final rolling temperature is 840°C. The elongation of hot rolled plates produced by DSCCR is over 35% and it is greater than the required value of 29%. The yield ratio varies from 0.79 to 0.83 at different temperatures and in different directions. Therefore, in order to obtain the hot rolled plate with relatively stable performance in all directions, the final rolling temperature should be above 840°C.

Plastic strain ratio ( $r$  value) reflects the ability of sheet metal to resist thinning or thickening when it is under tension or pressure in a plane. It is the most important parameter to evaluate the deep drawing performance of sheet metal. The  $r$  value deviating 0°, 45° and 90° from rolling direction are described by  $r_0$ ,  $r_{45}$  and  $r_{90}$  respectively. Because the texture structure and mechanical properties of the plate are inconsistent in different directions, the weighted average thickness anisotropy coefficient ( $r_m$ ) is used:

$$r_m = \frac{r_0 + 2r_{45} + r_{90}}{4} \quad (1)$$

The greater the  $r$  value, the greater the ability of the plate to resist instability and thinning, and the less likely it is to develop thick deformation; the smaller the  $r$  value, the weaker the ability

of the plate to resist instability and thinning, and the easier the thick deformation. If  $r = 1$ , it indicates that there is no thickness anisotropy in the plate.

Degree of planar anisotropy ( $\Delta r$ ) can be calculated by:

$$\Delta r = \frac{r_0 - 2r_{45} + r_{90}}{2} \quad (2)$$

The larger the value of  $\Delta R$ , the more serious the in-plane anisotropy of the sheet, which is manifested in uneven edges, ears and uneven side wall thickness after drawing, which affect the forming quality. Strain hardening index ( $n$  value) reflects the ability of metal materials to resist uniform plastic deformation. It is a performance index to characterize the strain hardening behavior of metal materials. The level of hardening index indicates the ability of materials to make uniform deformation by hardening before necking. If the  $n$  value is large, the machined parts have a relatively large ability to withstand accidental overload during service, which can prevent some weak areas of the parts from continuing plastic deformation. The strain hardening effect is high, the deformation is uniform, the thinning is reduced and the limit deformation degree is increased, it is not easy to produce cracks, and has excellent stamping performance.

The  $r$  and  $n$  of hot rolled plates at different final rolling temperatures are shown in Fig. 6. It can be seen that with the decrease of final rolling temperature,  $r_{45}$  is relatively stable around 0.9,  $r_{90}$  decreases significantly after 840°C, and  $r_0$  decreases slowly after 840°C.  $n$  value in the three directions tended to be consist-

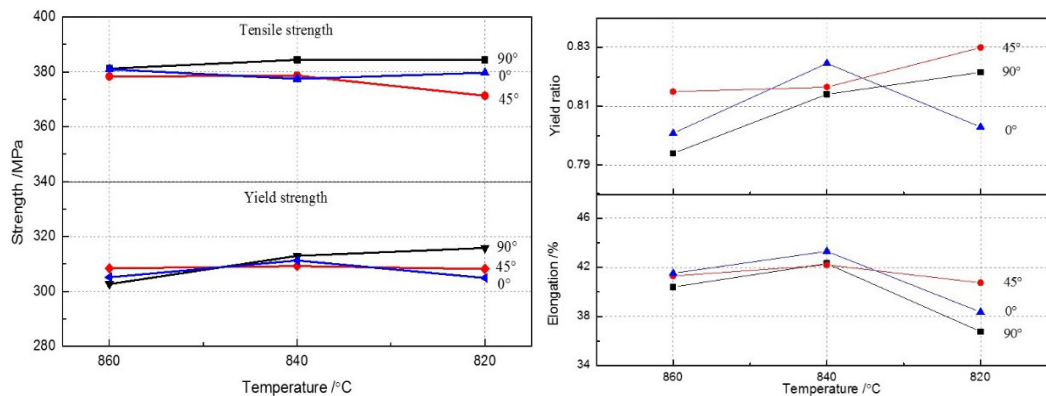


Fig. 5. Tensile properties at different final rolling temperatures

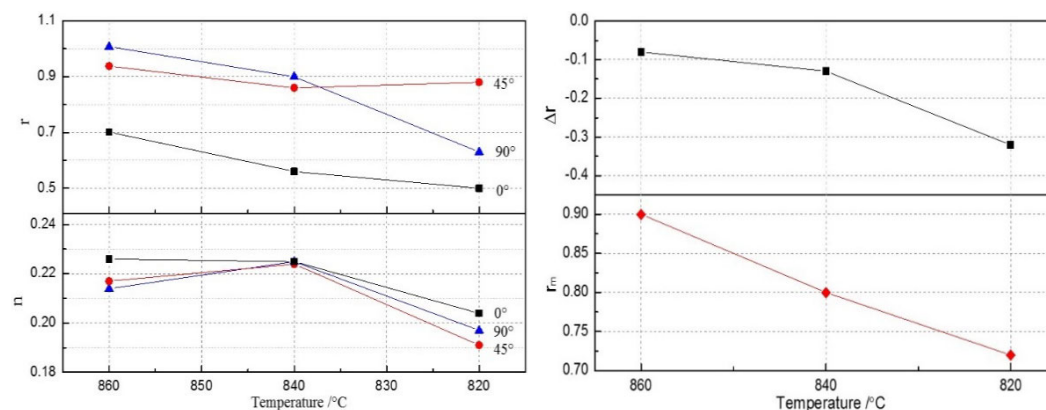


Fig. 6. The  $r$  and  $n$  of hot rolled plates at different final rolling temperatures

ent at 840°C and decreased significantly below 840°C.  $\Delta r < 0$  indicates that ear making mainly occurs in the direction of 45°.  $|\Delta r|$  increases with the decrease of final rolling temperature, and  $r_m$  decreases with the decrease of final rolling temperature, indicating that the formability becomes worse with the decrease of final rolling temperature. Relevant research [19] shows that for hot-rolled high strength low alloy steels produced by ESP,  $r_m$  was 0.7-0.9 and the greatest values of the  $r$  value was along the direction at 45° from the rolling one.

### 3.3. Texture characteristics at different final rolling temperatures

EBSM method is powerful tool for microstructural analysis of grains, grain boundaries, angular boundaries, twins, GAM, etc. [20]. EBSD method was used to analyze the texture of hot rolled plates at different final rolling temperatures. The grain orientation distribution map parallel to rolling direction is shown

in Figure 7, in which the blue, red and green indicate the normal direction of grains parallel to the  $\langle 111 \rangle$ ,  $\langle 001 \rangle$  and  $\langle 101 \rangle$  directions, respectively. The microstructure and grain distribution are consistent with Fig. 2. For 860°C, ferritic grains are relatively uniform, with an average grain size of 10.7  $\mu\text{m}$  and the average aspect ratio is 1.79. For 840°C, The average grain size of ferrite is about 8.2  $\mu\text{m}$  and significantly smaller than that of 860°C, the aspect ratio is 1.78, and there is a fine ferrite area near the surface. For 820°C, the average grain size of ferrite in the upper half (surface) is 12.5  $\mu\text{m}$  and its average aspect ratio is 1.77, but the average grain size of ferrite in the lower half (center) is 9.0  $\mu\text{m}$  and its average aspect ratio is 1.83. By comparing the microstructure of the upper and lower parts of ferrite, it can be seen that the grain size decreases due to deformation induced ferrite transformation, and the aspect ratio increases due to deformation in the two phase region, and the grain is coarse due to the pre eutectoid ferrite in the surface.

Fig. 8 shows the misorientation distribution of hot rolled plates at different final temperatures. It can be seen that the cor-

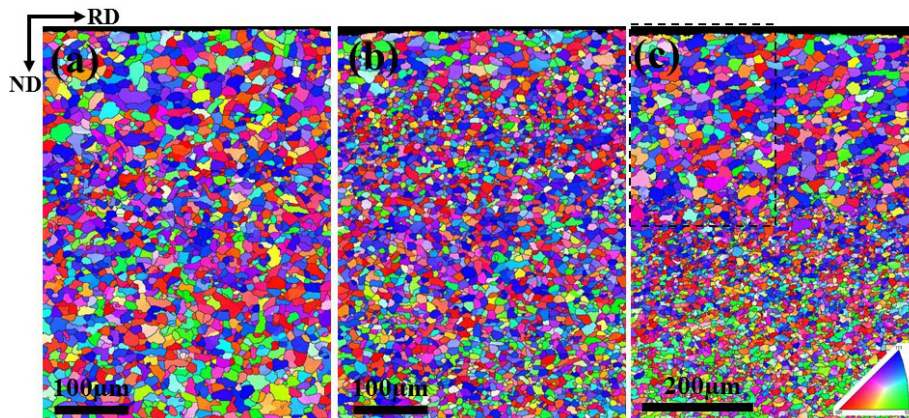


Fig. 7. The grain orientation distribution map parallel to rolling direction: (a) 860°C; (b) 840°C; (c) 820°C

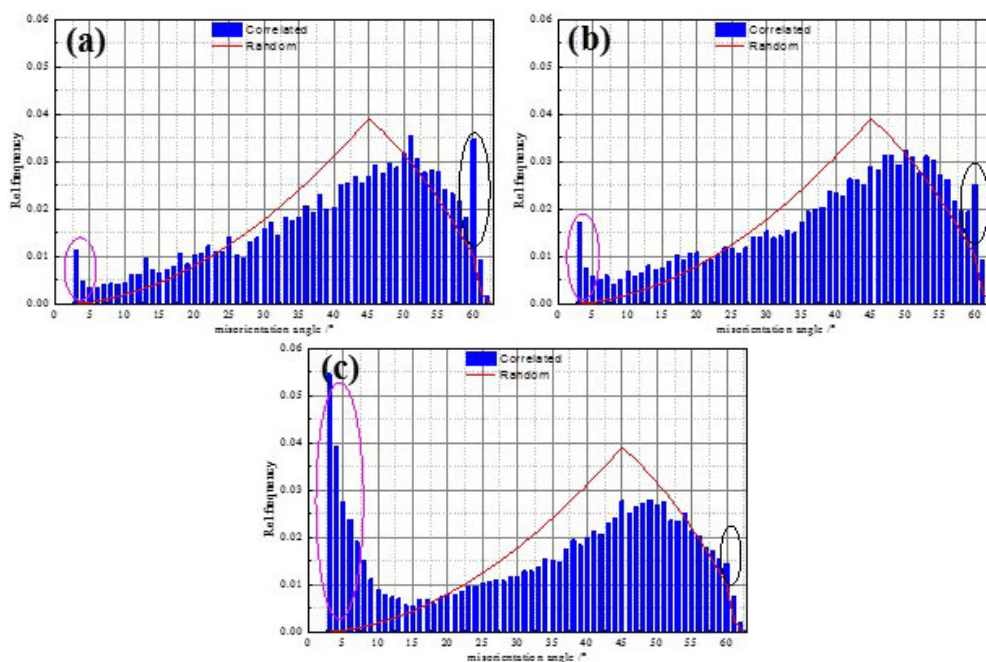


Fig. 8. Misorientation distributions at different rolling temperature: (a) 860°C; (b) 840°C; (c) 820°C

related misorientation distribution is generally consistent with the random misorientation distribution. It is considered that the hot rolled plate produced by DSCCR has no obvious misorientation as a whole, but there are significant differences in texture at different final rolling temperatures. The relative frequency of small angle grain boundary ( $<10^\circ$ ), especially sub grain boundary ( $<3^\circ$ , see the red ellipse) increases significantly with the decrease of final rolling temperature, while the relative frequency of near  $60^\circ$  (see the black ellipse) decreases significantly, indicating that there is a complementary relationship between the orientation below  $10^\circ$  and the orientation of  $60^\circ$ . Small angle reflects deformation degree and large angle grain boundary reflects recrystallization degree. It can be inferred that the recrystallization degree of hot rolled plate decreases and the deformation intensifies with the decrease of final rolling temperature.

In order to further observe the misorientation distribution of correlated grains, the small angle grain boundary distribution of hot rolled plates with different final rolling temperatures is shown in Fig. 9, in which the green line represents the grain boundary of the misorientation  $<10^\circ$  and the black line represents the large angle grain boundary. It can be seen that small angle grain boundaries are few and randomly distributed at the final rolling temperature of  $860^\circ\text{C}$ . For  $840^\circ\text{C}$ , the small angle grain boundaries increase, but the distribution is still random. For  $820^\circ\text{C}$ , the small angle grain boundaries increased significantly

and mainly distributed in the lower half of the small grain area. However, no obvious increase of small angle grain boundaries was found in the near surface fine grain area at  $840^\circ\text{C}$ .

In order to further study the relationship between grain type and small angle grain boundary, the recrystallization analysis of hot rolled plates at different final rolling temperatures is carried out, and the distribution of recrystallized grains is shown in Fig. 10, in which the blue, yellow and red color represent recrystallized grains, substructure grains and deformed grains, respectively. When the final rolling temperature is  $860^\circ\text{C}$ , the substructure grains and deformed grains are randomly distributed, and the proportions of recrystallized grains, substructure grains and deformed grains are 83.4%, 15.1% and 1.5%, respectively. When the final rolling temperature is decreased to  $840^\circ\text{C}$ , the substructure grains and deformed grains are still randomly distributed, but the substructure grains are finer, and the deformed grains increase significantly. The proportions of recrystallized grains, substructure grains and deformed grains are 72.5%, 18.7% and 8.8%, respectively. When the final rolling temperature is further reduced to  $820^\circ\text{C}$ , the small angle grains increase greatly, while the recrystallized grains and substructure grains decrease. The small angle grains are mainly distributed in the fine grain region in the lower half, and the substructure grain distribution density in the coarse and fine grain transition region is lower than  $840^\circ\text{C}$ . The proportions of recrystallized grains,

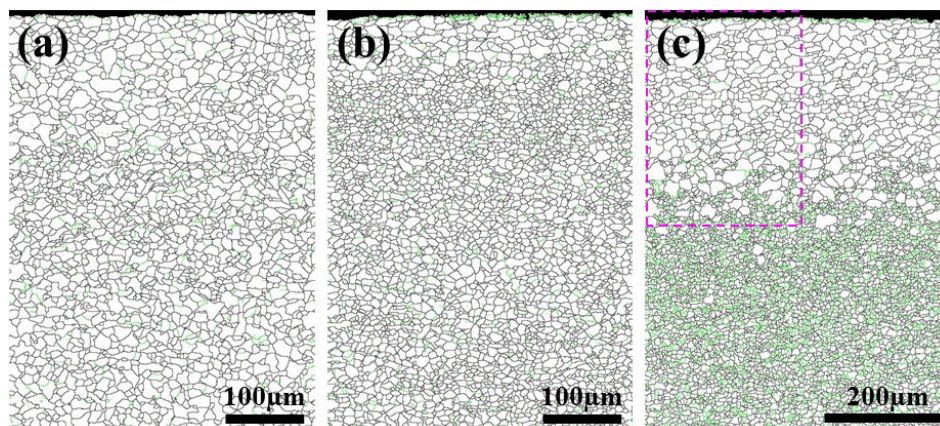


Fig. 9. Distribution of the grain boundaries at different final rolling temperature: (a)  $860^\circ\text{C}$ , (b)  $840^\circ\text{C}$ , (c)  $820^\circ\text{C}$

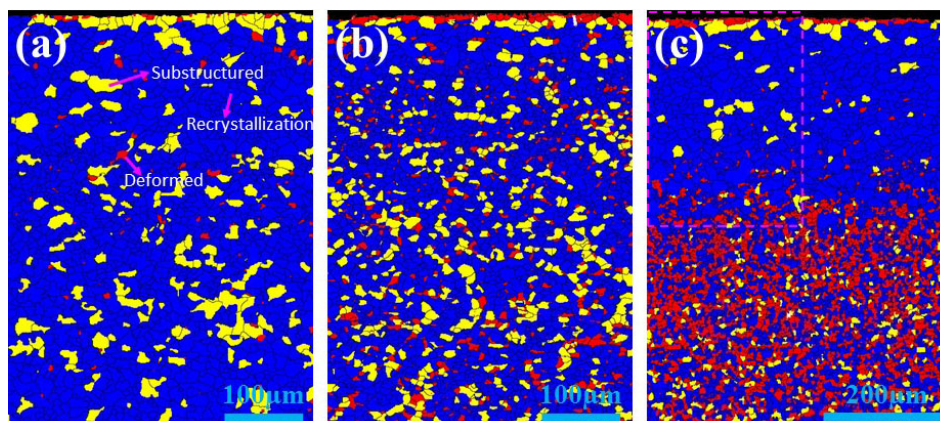


Fig. 10. Distribution of recrystallized grains at different final rolling temperature: (a)  $860^\circ\text{C}$ , (b)  $840^\circ\text{C}$ , (c)  $820^\circ\text{C}$

substructure grains and deformed grains are 68.0%, 8.3% and 23.7%, respectively. It further shows that the deformed grain in the fine grain region is deformation induced ferrite, and the recrystallized grain is transformed from deformed austenite. Reference [21] holds that due to large deformation, a large amount of internal stress is accumulated, although most of the internal stress will be released during grain growth, a large amount of residual internal stress is still retained in the material, excessive grain refinement does not necessarily bring great benefits. Therefore, it is considered that the significant increase proportion of deformed ferrite grain at the center of the steel strip is the main factor causing the decrease of elongation when the final rolling temperature is 820°C. The dislocation model considers that low angle grain boundaries (LAGB) can be regarded as a series of dislocations. The more LAGB, the higher the dislocation density and the more distortion energy. When the final rolling temperature is in the two-phase region, the pre-eutectoid ferrite is deformed by the rolling force and becomes deformed ferrite with high dislocation density and high grain boundary energy (red parts in the lower part of Fig. 10c), but the grain boundary energy is low for the fine equiaxed ferrite formed by deformed austenite transformation. At the same time, due to rolling friction, the distribution of shear strain in the workpiece is not uniform, the further away from the surface, the smaller the strain. When the interface energy difference between the two sides of the grain boundary reaches a critical value, the migration of the grain boundary occurs, that is, the pre-eutectoid ferrite engulfs the fine ferrite transformed by deformed austenite, the surface grains grow and change into recrystallized grains (blue grains on the surface in Fig. 10c).

### 3.4. Hole expanding behaviors at different final rolling temperatures

The hole expanding morphology of hot rolled plate at different final rolling temperatures is shown in Fig. 11. It can be seen that the damage mode is  $\beta$  fracture caused by insufficient elongation. The limiting hole expansion ratios at different final rolling temperatures are 129%, 121% and 122%, respectively, indicating that the remaining formability of hot rolled plates is similar during this final rolling temperature range.

### 3.5. Earing behaviors at different final rolling temperatures

Fig. 12 shows the photograph of draw cups and earing expansion from rolling direction at different final rolling temperatures. It can be seen that the earing of hot rolled plate at final rolling temperature of 860°C is not obvious, but there are relatively obvious earing at the final rolling temperatures of 840°C and 820°C, and the ears appear at the direction of 45°. Relevant studies [12] also show that the cup height was high in the 45 degree direction in the low carbon steels produced by the CEM process and conventional continuous-casting and hot-rolling process. In order to quantitatively describe the characteristics of earing behaviors, Several important indexes to characterize the earing propensity are listed in TABLE 2, in which  $\bar{h}_t$ ,  $\bar{h}_v$ ,  $\bar{h}_e$ ,  $\Delta h_{max}$ , and  $Z_e$  are used to describe the average height of ear peak, ear valley, earing, maximum ear height, and earing coefficient, respectively. TABLE 2 shows several important

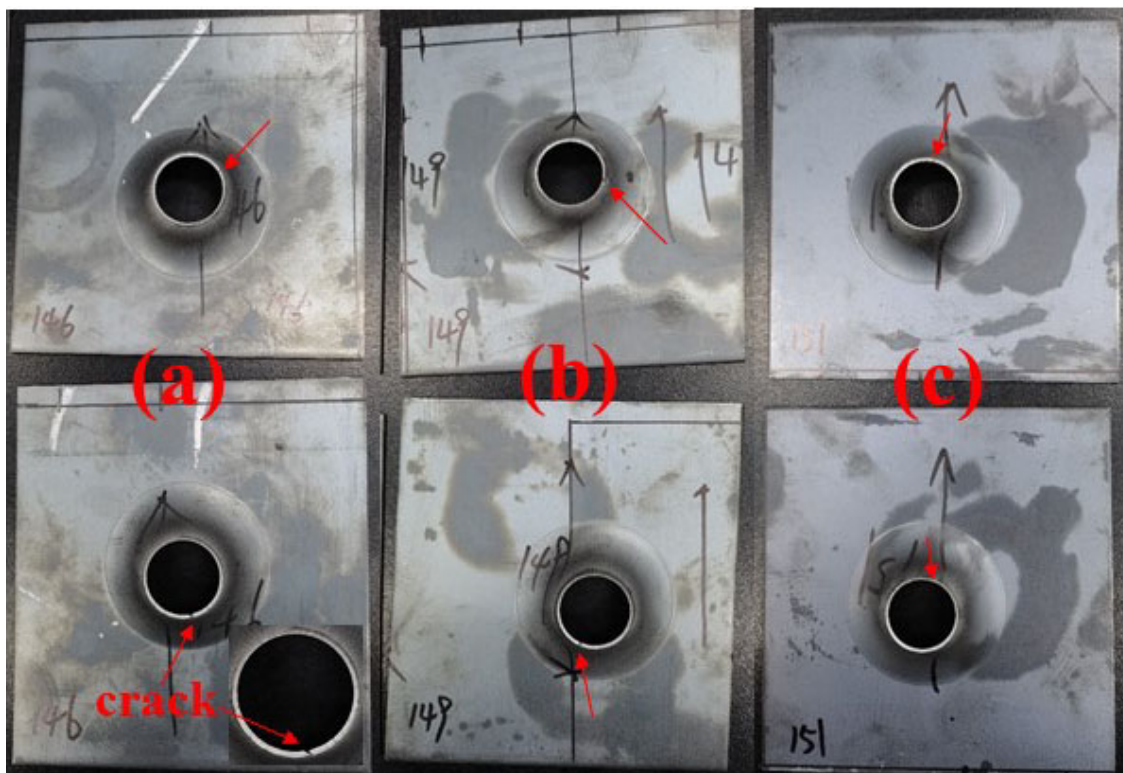


Fig. 11. Hole expanding morphology at different final rolling temperature: (a) 860°C, (b) 840°C, (c) 820°C

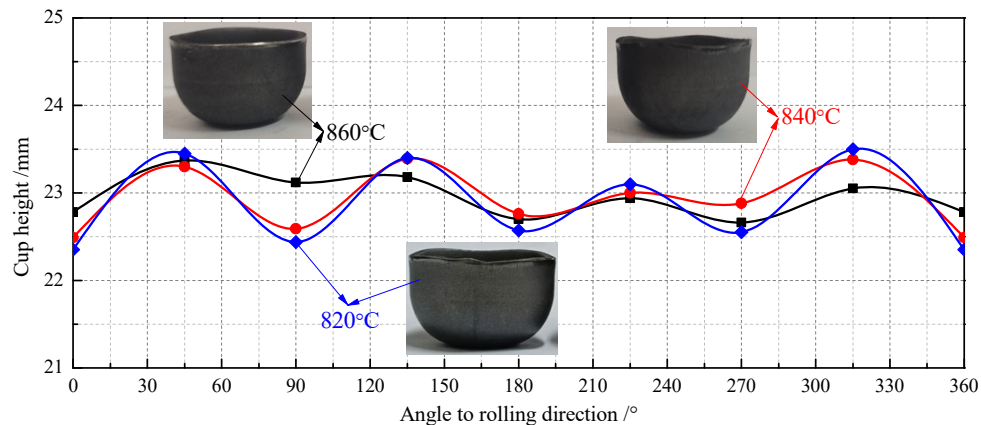


Fig. 12. Photograph of draw cups and earing expansion from rolling direction

indicators describing the characteristics of ear making, including  $Ze$  and  $\Delta h$  is used to reflect the plastic plane anisotropy of metal sheet. It can be seen that with the decrease of final rolling temperature,  $\bar{h}t$ ,  $e$ ,  $\Delta h_{max}$  and  $Ze$  increase, indicating that the anisotropy increases, which is consistent with the results in Fig. 6.

TABLE 2

Several important indexes to characterize the earing propensity

CT (°C)	$\bar{h}t$ (mm)	$\bar{h}v$ (mm)	$\bar{h}e$ (mm)	$\Delta h_{max}$ (mm)	$Ze$ (%)	Earing Direction (°)
860	23.14	22.82	0.32	0.71	1.40	45
840	23.27	22.68	0.59	0.90	2.59	45
820	23.36	22.48	0.88	1.15	3.94	45

In conclusion, when the final rolling temperature is 860°C, because the residence time in laminar cooling process is less than 10 s, so the austenite transformation happens in the subsequent laminar cooling and coiling process, and a small amount of  $Fe_3C_{III}$  begins to precipitate when the temperature is lower than  $A_1$ . Its microstructure includes massive proeutectoid ferrite, equiaxed eutectoid ferrite, lamellar pearlite and rod cementite. Because of its uniform microstructure along the thickness and large grain size, its  $r$  was higher and  $\Delta r$  was smaller, so good formability could be obtained, its limiting hole expansion ratios and earing propensity were the best. When the final rolling temperature is 840°C, it enters the temperature zone of deformation induced ferrite transformation, a small amount of fine deformation induced ferrite grains are preferentially precipitated at the original austenite grain boundary. A large amount of deformed austenite undergo ferrite transformation during the laminar cooling and coiling process, and a small amount of  $Fe_3C_{III}$  begins to precipitate when the temperature is lower than  $A_1$ . Its microstructure includes a small amount of fine deformation induced ferrite and proeutectoid ferrite, massive equiaxed eutectoid ferrite, lamellar pearlite and rod cementite. Due to the existence of fine equiaxed deformation induced ferrite and narrow lamellar pearlite, it has better plasticity and toughness, so its elongation are the best. When the final rolling temperature is 820°C, it enters the dual phase zone of austenite and ferrite, a large

amount of proeutectoid ferrite is deformed to become deformed ferrite, a small amount of deformed austenite undergoes ferrite transformation during the laminar cooling and coiling process, and a small amount of  $Fe_3C_{III}$  begins to precipitate when the temperature is lower than  $A_1$ . Its microstructure includes a large amount of deformed ferrite, equiaxed eutectoid ferrite, lamellar pearlite and rod cementite, the surface ferrite recrystallizes and grows into large-size recrystallized ferrite because the action of shear stress caused by friction. Due to the existence of a large number of small deformed ferrite and mostly small angle grain boundary at their grain boundaries, the elongation and the earing propensity declined rapidly. However, because the surface layer was a coarse grain region, the limiting hole expansion ratios changed little. However how to distinguish the different ferrite types in the above theory needs to be further studied. It is worth noting that even the final rolling temperature is decreased from the conventional austenite zone rolling temperature ( $\geq 880^\circ C$ ) to the ferrite and austenite temperature region (820°C), the elongations, limiting hole expansion ratios and earing coefficients of 2.0 mm thick hot-rolled plate produced by DSCCR line are respectively greater than the procurement requirements of 27%, 100% and 5%, so its performance meets the requirements of hot rolled plate replacing cold rolled plate.

#### 4. Conclusions

In this research, 2.0 mm thickness hot rolled plate produced by DSCCR line at different final rolling temperatures was studied, and a detailed investigation of the microstructural evolution, mechanical properties, texture characteristics by EBSD, and formability including hole expanding ratio and earing behavior was carried out. The following conclusions can be drawn:

- (1) The results show that with the decrease of final rolling temperature, there is an obvious layered microstructure distribution along the thickness direction, and the surface coarse grain area gradually expands inward, at the same time the morphology of cementite also changed from large multi domain lamellar pearlite and long rod cementite to small single domain lamellar pearlite and short rod cementite.

- (2) The engineering stress-strain curves have discontinuous yield with the yield elongation of 4-5% and the elongations are more than 35%. with the decrease of the final rolling temperature, the anisotropy of hot rolled plate is more obvious and the formability decreases, the final rolling temperature has a certain impact on the microstructure and properties because the phase transition mechanism is closely related to the transition temperature.
- (3) EBSD analysis shows that small angle grain boundaries and deformed grains increase significantly with the decrease of final rolling temperature, and are mainly distributed in fine grain area. Hole expanding and earing tests show that with the decrease of final rolling temperature, the earing performance decreased but the limiting hole expanding ratio is similar.
- (4) In short, the final rolling temperature is decreased from the conventional austenite zone rolling temperature ( more than 860°C) to the ferrite and austenite temperature region (820°C), its performance meets the requirements of hot rolled plate replacing cold rolled plate.
- [4] Y. Ma, N. Li, T. Yang, Hebei Metallurgy **4** (06), 37-40 (2021).
- [5] Y.L. Kang, P. Tian, G.M. Zhu, Iron Steel **54**, 1-8 (2018).
- [6] B. Linzer, J. Andreas, Materials Science Forum **854**, 207-214 (2016).
- [7] P. Tian, Y.L. Kang, G.M. Zhu, et al., Materials Science Forum **4734**, 344-350 (2019).
- [8] K. Liu, C. Ji, S. Wang, et al. Journal of Iron and Steel Research **33** (02), 143-148 (2021).
- [9] Q. Tang, G. Niu, H. Wu, et al., Metals **11** (251), 1-13 (2021).
- [10] R. Venturini, P. Avancini, N. Barbier, et al., Materials Science Forum **4190**, 42-47 (2016).
- [11] V. Naumenko, O. agmet, M. Matrosov, et al., Steel in Translation **50** (7), 501-508 (2020).
- [12] J.W. Bae, H.Y. Um, S.H. Lee, et al., Metallurgical & Materials Transactions A **48** (3), 1021-1032 (2017).
- [13] P. Tian, G.M. Zhu, Y.L. Kang, Materials **14**, 1-20 (2021).
- [14] F. Wang, P. Tian, Y.L. Kang, et al., Materials Science Forum **4734**, 329-336 (2019).
- [15] X. Hu, G. He, Y. Li, et al., Heat Treatment of Metals **44** (10), 56-60 (2019).
- [16] W. Hui, P. Tian, H. Dong, et al., Acta Metallurgica Sinica (06), 611-616 (2005).
- [17] G. Jung, Y. Ho, Y. Ji, et al., Mater. Sci. Eng. A **734**, 408-415 (2018).
- [18] J. Hallai, S. Kyriakides, Int. J. Plast. **47**, 1-12 (2013).
- [19] A. Guindani, R. Venturini, C. Mapelli, et al., Metall. Ital. (1), 25-30 (2014).
- [20] M. Černík, R. Gburík, L. Hrabčáková, et al., IOP Conf. Ser.: Mater. Sci. Eng. **82** (17), 24-29 (2015).
- [21] Y.Q. Weng, Ultra-Fine Grained Steels, Metallurgical Industry Press 1 (2008).

## REFERENCES

- [1] G. Arvedi, F. Mazzolari, J. Siegl, et al., Ironmak. Steelmak **37**, 271-275 (2010).
- [2] K. Hoen, C. Klein, S. Krämer, et al., BHM Bergund Hüttenmännische Monatshefte **161** (9), 415-420 (2016).
- [3] A. Pigani, P. Bobig, M. Knights, et al., Bergund Hüttenmännische Monatshefte **161** (9), 429-439 (2016).